Universal Knight shift anomaly in the periodic Anderson model

M. Jiang, N. J. Curro, and R. T. Scalettar

Universal Knight shift anomaly in the Periodic Anderson model

M. Jiang[1,2], N.J. Curro,[1] and R.T. Scalettar[1]

[1]*Physics Department, University of California, Davis, California 95616, USA and*
[2]*Department of Mathematics, University of California, Davis, California 95616, USA*

We report a Determinant Quantum Monte Carlo investigation which quantifies the behavior of the susceptibility and the entropy in the framework of the periodic Anderson model (PAM), focussing on the evolution with different degree of conduction electron (c) -local moment (f) hybridization. These results capture the behavior observed in several experiments, including the universal behavior of the NMR Knight shift anomaly below the crossover temperature, T^*. We find that T^* is a measure of the onset of c-f correlations and grows with increasing hybridization. These results suggest that the NMR Knight shift and spin-lattice relaxation rate measurements in non-Fermi liquid materials are strongly influenced by the temperature-dependence of the c-f kinetic energy. Our results provide a microscopic basis for the phenomenological two-fluid model of Kondo lattice behavior, and its evolution with pressure and temperature.

Heavy-fermion materials have attracted considerable attention over the past two decades because of their unusually large effective masses arising from strong electron correlations [1, 2]. These materials, which typically contain either Ce, Yb, U or Pu ions, exhibit complex behaviors arising from the interplay between localized and itinerant electrons. In some cases these interactions lead to ordered ground states such as superconductivity, antiferromagnetism, or more exotic "hidden" order [3, 4]. In other cases the strong correlations lead to a breakdown of conventional Fermi-liquid theory in proximity to a quantum phase transition [5–7]. The recent discovery of the CeMIn$_5$ (M = Rh, Ir, or Co) class of heavy fermions, which exhibit a broad spectrum of unusual ground states accompanied by quantum criticality and non-Fermi liquid behavior, has highlighted the continued need to develop a general understanding of the phase diagram of heavy fermions, as well as a requirement to discern what behaviors are universal rather than material-specific [8–10].

Among various experimental techniques used to investigate heavy fermion materials, nuclear magnetic resonance (NMR) plays a central role [11]. Because the hyperfine coupling between nuclear and electron spins introduces an additional local effective field at the nucleus, NMR allows one to probe the relative shift of the nuclear resonance frequency compared with the same nucleus in isolation. In a normal Fermi liquid, the Knight shift is given $K = A\chi_0/\hbar\gamma\mu_B$, where χ_0 is the Pauli susceptibility proportional to the density of states at the Fermi level, so that $K \propto AN(0)$ is temperature independent. On the other hand, this scenario fails to describe the non-Fermi liquid behavior in the normal state of heavy fermion materials, in which the magnetic susceptibility χ usually increases strongly with decreasing temperature. Below a particular crossover temperature $T^* \sim 10 - 100$ K, the Knight shift K is no longer proportional to the magnetic susceptibility,

reflecting the onset of hybridization or lattice coherence between conduction electron and the local moment f-electrons. This Knight shift anomaly has been detected in all heavy fermion materials that have been measured, including the CeMIn$_5$ family, CeCu$_2$Si$_2$, UPt$_3$, and URu$_2$Si$_2$ [12, 13].

A variety of different hypotheses have been put forward to explain the origin of the Knight shift anomaly, which either argue that the hyperfine interaction acquires a temperature dependence due to Kondo screening [15], or attributes the effect to different occupations of crystal field levels of the 4f(5f) electrons in these materials [16]. However, if the hyperfine coupling has much larger energy scale than the Kondo and/or crystal field interactions it is challenging to reconcile that they should give rise to the dramatic changes observed experimentally [17].

Recent progress has emerged in the context of a two-fluid model, in which localized f-electron spins and itinerant conduction electron spins interact with the nuclear spins via two different hyperfine couplings [18, 20–23]. The two-fluid picture has attracted much interest as a promising phenomenological model of several heavy-fermion behaviors, but a connection of the predictions of this theory to a microscopic many-body Hamiltonian is needed to provide a more comprehensive, and quantitative understanding.

It is well known that much of heavy fermion physics can be captured by the Kondo lattice model and/or periodic Anderson model (PAM) [24] in which a lattice of f-electron local moments is embedded into a background of conduction electrons. As the hybridization between conduction and localized f-electrons, repulsive interaction U_f for localized moments, and the temperature are varied, there is a competition between singlet formation by the Kondo effect and antiferromagnetism favored by the Ruderman-Kittel-Kasuya-Yosida (RKKY) interaction [25]. It is natural to consider whether these microscopic models might also

be used to understand the Knight shift anomaly.

We employ the PAM to investigate the Knight shift anomaly observed in NMR studies of several heavy fermion materials. The Hamiltonian reads:

$$\mathcal{H} = - t \sum_{\langle ij \rangle, \sigma} (c_{i\sigma}^\dagger c_{j\sigma} + c_{j\sigma}^\dagger c_{i\sigma}) - V \sum_{i\sigma} (c_{i\sigma}^\dagger f_{i\sigma} + f_{i\sigma}^\dagger c_{i\sigma})$$
$$+ U_f \sum_i (n_{i\uparrow}^f - \frac{1}{2})(n_{i\downarrow}^f - \frac{1}{2}) \qquad (1)$$

where $c_{i\sigma}^\dagger (c_{i\sigma})$ and $f_{i\sigma}^\dagger (f_{i\sigma})$ are creation(destruction) operators for conduction and local electrons on site i with spin σ. $n_{i\sigma}^{c,f}$ are the associated number operators. Here the chemical potential and f electron site energy $\mu = E_f = 0$, and both bands are individually half-filled. t is the hopping between conduction electrons on near neighbor sites $\langle ij \rangle$ of a square lattice, U_f the local repulsive interaction in the f orbital and V the hybridization between conduction and localized electrons. $t = 1$ sets the energy scale. Results shown here are for a 2D square lattice but are qualitatively unchanged in 3D, as discussed below and in [26].

The PAM exhibits two distinct low temperature magnetic phases [27]. For small V, local f moments couple antiferromagnetically via an indirect RKKY interaction mediated in the conduction band. At large V, conduction and local electrons lock into independent singlets, and a paramagnetic spin liquid ground state forms. This reflects a competition between the RKKY and Kondo energy scales, $\sim J^2/W$ and $\sim We^{-W/J}$, respectively, with $J \sim V^2/U_f$ and W the bandwidth.

We solve the PAM and address the Knight shift anomaly problem by using Determinant Quantum Monte Carlo (DQMC) [28]. In this method, a path integral expression is written for the quantum partition function $\mathcal{Z} = \text{Tr} \exp(-\beta \mathcal{H})$, the interaction term $n_{i\uparrow}^f n_{i\downarrow}^f$ between localized f electrons is isolated, and then mapped onto a coupling of the f electron spin with a space and imaginary-time dependent auxiliary ("Hubbard-Stratonovich") field $S_{i\tau}(n_{i\uparrow}^f - n_{i\downarrow}^f)$. After this replacement, which treats the interaction energy without approximation [29], the fermionic degrees of freedom can be integrated out analytically. The result is an exact expression for $\mathcal{Z}$ and operator expectation values for spin, charge, and pairing correlation functions in terms of integrals over the field configurations $\{S_{i\tau}\}$. Summing these correlation functions over different spatial and imaginary-time separations yields the magnetic and superfluid susceptibilities, and the charge compressibility which signal the onset of different ordered phases. For the half-filled case of Eq. 1, the sampling is over a positive-definite weight [30], and expectation values can be obtained to low temperatures.

In the two-fluid theory [13, 18] the nuclear moment $\vec{I}$ experiences hyperfine interactions with both the conduction and localized electron spins $\vec{S}_i^c =$
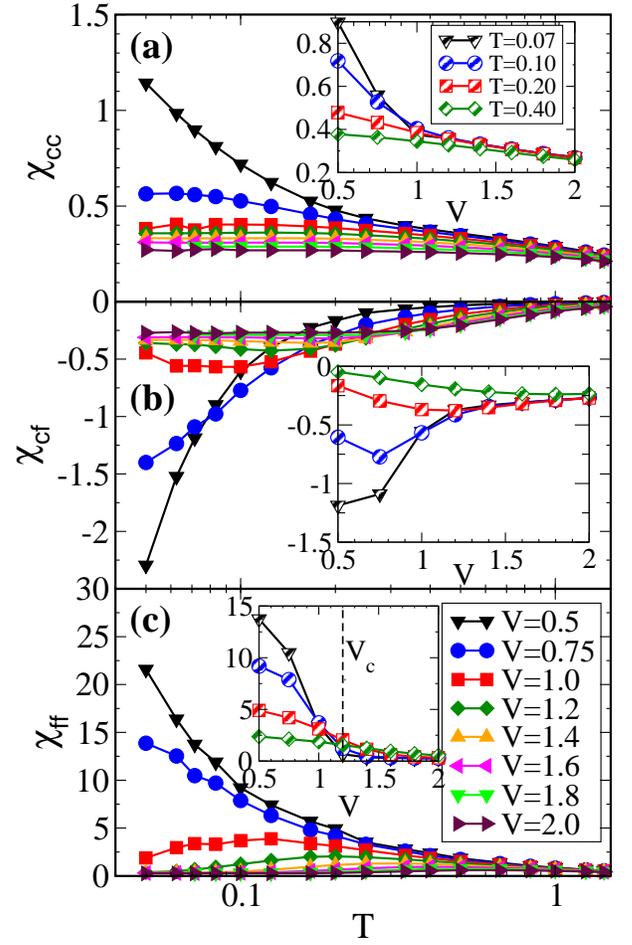
FIG. 1: (Color online) Evolution of the three components of the uniform ($q = 0$) magnetic susceptibility with temperature T (main panels) and inter-orbital hybridization V (insets). At weak V, the conduction and local f electrons decouple, exhibiting Pauli and Curie behavior respectively. All three susceptibilities fall as V increases and Kondo singlets form, becoming small and temperature independent in the vicinity of the AF-singlet transition at $(V/t)_c \sim 1.2$ (vertical dashed line in panel (c) inset). See [25]. Here the on-site repulsion of the local orbital is $U_f = 4$ and the lattice size is 12×12. (Discussion of finite size effects is contained in the Supplemental Materials.)

$(c_{i\uparrow}^\dagger c_{i\downarrow}^\dagger)\vec{\sigma} \begin{pmatrix} c_{i\uparrow} \\ c_{i\downarrow} \end{pmatrix}$ and $\vec{S}_i^f = (f_{i\uparrow}^\dagger f_{i\downarrow}^\dagger)\vec{\sigma} \begin{pmatrix} f_{i\uparrow} \\ f_{i\downarrow} \end{pmatrix}$ via $\mathcal{H}_{\text{hyp}} = \vec{I}_i \cdot (A\vec{S}_i^c + B\vec{S}_i^f)$. Here A and B are the associated hyperfine couplings and include also proportionality constants $\gamma\hbar g\mu_B$, and $\vec{\sigma}$ are the Pauli matrices. If the electronic spins are polarized via an external magnetic field H, then $S_i^c = (\chi_{cc} + \chi_{cf})\text{H}$ and $S_i^f = (\chi_{cf} + \chi_{ff})\text{H}$, so that the magnetic susceptibility and Knight shift are

$$\chi = \chi_{cc} + 2\chi_{cf} + \chi_{ff}$$
$$K = A\chi_{cc} + (A+B)\chi_{cf} + B\chi_{ff} + K_0 \qquad (2)$$

respectively. K_0 is a temperature independent term arising from orbital and diamagnetic contributions to K.
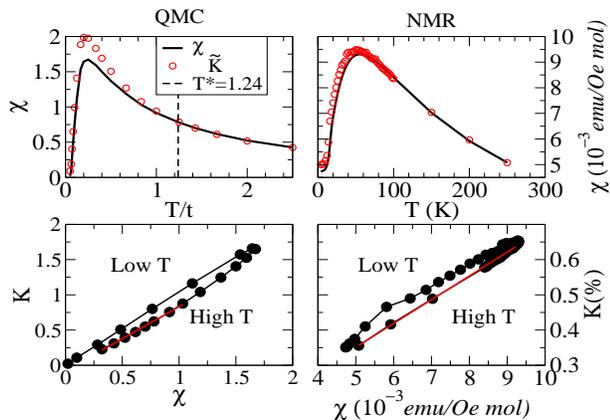
FIG. 2: (Color online) Analysis of the Knight shift anomaly. Left panels are DQMC data for the PAM at $V = 1.2$ and $U_f = 4$. Right-hand panels are experimental data on URu$_2$Si$_2$. Both DQMC and experimental data for $T > T^*$ can be fit with a straight line $K = B_{\rm eff} \chi + K_{0\,\rm eff}$ [32]. Top panels: Susceptibility χ and renormalized Knight shift $\tilde{K} = (K - K_{0\,\rm eff})/B_{\rm eff}$ as functions of temperature. Above the coherence temperature, $T > T^*$, $\tilde{K}$ tracks χ. Below T^*, the Knight shift anomaly is evident in a deviation of $\tilde{K}$ from χ. The bottom panels show K versus χ with T as an implicit parameter [19]. The hyperfine couplings $A = 0.3, B = 1.0$, and $K_0 = 0.0$.

If $A \neq B$, the different weights of the three components of the total susceptibility and their different temperature dependencies results in a breakdown of the linear relation between K and χ for $T < T^*$.

To quantify the Knight shift anomaly and the possibility of universal behavior, we obtain, by summing over appropriately restricted sets of orbitals, the three components, χ_{cc}, χ_{cf}, and χ_{ff}, shown in Fig. 1. When V is small, the PAM describes noninteracting conduction electrons decoupled from free moments. At low temperature, χ_{cc} is expected to approach a T-independent Pauli limit, while χ_{ff} should have a Curie-like divergence. This indeed qualitatively describes [31] the behavior at $V = 0.50$ and $V = 0.75$ in panels (a) and (c). The inter-orbital susceptibility χ_{cf}, panel (b), is negative, reflecting the tendency of the conduction and f moments to anti-align (which for large V results in singlet formation). Note that in the singlet phase the local, on-site contribution to χ_{cf}, $\langle \vec{S}_i^c \cdot \vec{S}_i^f \rangle$, is large. However, because the singlets are independent on different lattice sites, the nonlocal contributions $\langle \vec{S}_j^c \cdot \vec{S}_i^f \rangle$ for $i \neq j$ are reduced, leading to a small χ_{cf} at large V. For $U_f = 4$ it is known [25] that the antiferromagnetic to singlet transition occurs for $(V/t) \gtrsim 1.2$. This transition is reflected in the susceptibility components becoming temperature independent. (See vertical dashed line in inset to Fig. 1(c).)

The bottom panels of Fig. 2 show the Knight shift K as a function of susceptibility χ with T as an implicit
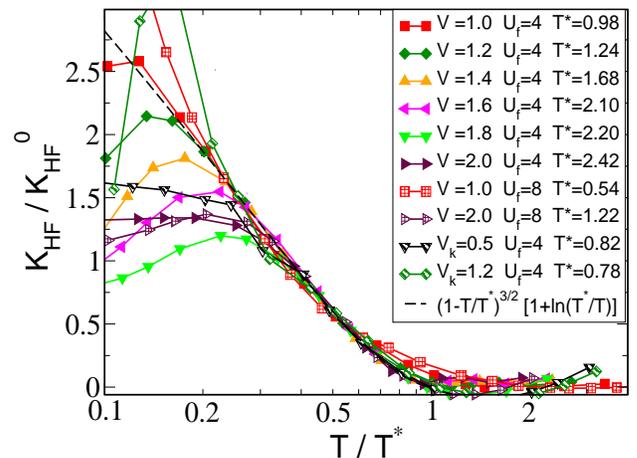
FIG. 3: (Color online) Knight shift data from DQMC simulations of the PAM are shown to exhibit a universal logarithmic divergence with decreasing temperature below T^* in the paramagnetic state. QMC data are fitted for a range of high temperatures with the relation Eq. 3. Universality is seen both for different V at fixed $U_f = 4$, as well as for two values of U_f and near-neighbor (k-dependent) hybridization $V_k(\cos k_x + \cos k_y)$. The breakdown of the scaling behavior of $K_{\rm HF}$ at the lowest temperatures is also seen experimentally and has been suggested to arise from "relocalization." See text for details. We have chosen the hyperfine couplings ratio $A = 0.3, B = 1.0$, but the universality is not dependent on details of the hyperfine coupling values. The dashed line is given by Eq. 3.

parameter. The strong qualitative similarity between PAM simulations (left panels) and the experimental data (right panels) in URu$_2$Si$_2$ [13] is evident. Note the $K - \chi$ plot bends counter-clockwise as T is lowered, however the magnitude and direction of this effect depends on the particular magnitudes of the hyperfine couplings, A and B. Similar plots with different values of V are available in the supplemental information.

NMR experimental results on several different families of heavy fermion compounds have revealed that the contribution to the Knight shift from the heavy electrons exhibits a *universal* logarithmic divergence with decreasing temperature below T^* in the paramagnetic state [12, 13]. The two-fluid model explains this observation by arguing that the Knight shift component from hybridized heavy fermions $K_{\rm HF} = K - (K_{0\,\rm eff} + B_{\rm eff}\chi)$ is proportional to the susceptibility of the heavy electron fluid, and can be described empirically as:

$$K_{\rm HF}(T) = K_{\rm HF}^0 (1 - T/T^*)^{3/2}[1 + \ln(T^*/T)] \quad (3)$$

where $K_{\rm HF}^0$ and the coherence temperature T^* are material-dependent constants [14]. In Fig. 3 we demonstrate that the predictions of this two-fluid picture, and NMR experimental results, can also be captured in a microscopic many-body Hamiltonian. Specifically, if we fit our QMC data for the Knight shift $K(T)$ in
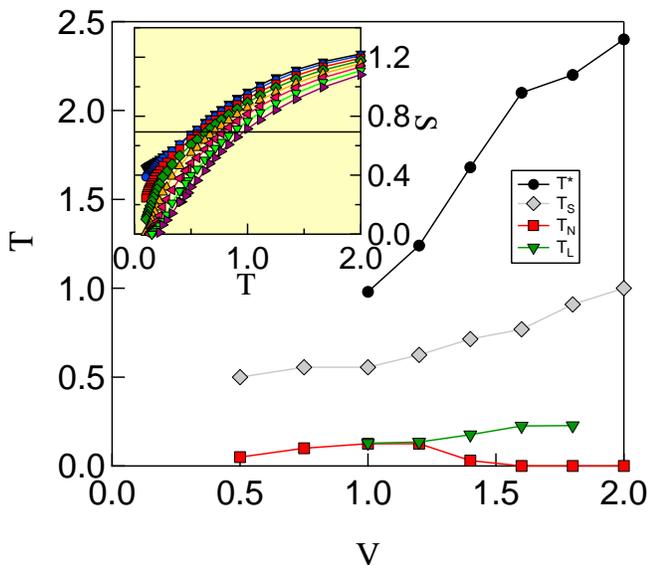
FIG. 4: (Color online) Evolution of T^*, T_S (the temperature at which $S = \ln 2$), T_{loc} and T_N with hybridization, V, where T_N is defined as the temperature where the antiferromagnetic correlation length exceeds the system size (note that $T_N = 0$ in 2D). (Inset) The thermodynamic entropy versus the temperature for different hybridization strength V (symbols and colors are defined in Fig. 1). With increasing V, the temperature at which the entropy decreases to the value $\ln 2$ increases. This is consistent with the expectation that around the crossover temperature T^* the hybridization between the conduction and localized f-electrons results in coherence between these degrees of freedom.

the PAM, allowing K_{HF}^0 and T^* to be free parameters, we find $K_{HF}(T)$ is universal over the range $0.2T^* < T < T^*$. Fig. 3 shows a scaling collapse for a range of conduction-local electron hybridizations V at fixed $U_f = 4$ and hyperfine couplings $A = 0.3, B = 1.0$. This universality persists when U_f is increased to $U_f = 8$ and for a modified form of V in which the local f orbitals are hybridized with conduction orbitals on *neighboring* lattice sites so that $V \rightarrow V_k (\cos k_x + \cos k_y)$. This latter choice emphasizes the universal scaling is insensitive to details of the band structure and bandwidth [33]. We have also verifgied that similar collapse behavior is exhibited for the 3D PAM. These data are shown in the supplemental materials.

The f electron density of states of the PAM at half-filling exhibits a sharp Mott transition at low temperatures[34, 35], a feature not accounted for in the two-fluid picture. However, for the choices of hybridization and temperature of Fig. 3, a gap in the f electron density of states is not present[35], so that the data lie within the regime where the half-filled PAM is an appropriate microscopic model. Doping the PAM would extend this regime of validity but is a challenge for DQMC simulations.

In addition to the demonstration of universality within a microscopic model, other features in the model agree with experimental observations. As shown in Fig. 4, (i) T^* increases with increasing V, and (ii) the scaling behavior of K_{HF} breaks down below a lower temperature $T_{loc} \sim T^*/5$. Although this latter behavior is not fully understood, it has been proposed that it is associated with the "relocalization" of f-electrons observed in materials like $CePt_2In_7$ whose ground states are antiferromagnetic [36]. In these materials, the finite value of K_{HF} at T_N suggests that the ordered local moments remain partially screened, emphasizing a continued competition between the heavy-fermion Kondo liquid and a hybridized "spin liquid" with a lattice of local moments associated with f-electrons [18]. Because T^* is an approximate measure of the onset of coherence between the itinerant and localized electrons, the two-fluid theory argues that the entropy at the crossover temperature $T^\star$ approaches $\ln 2$ at this temperature [14]. The inset of Fig. 4 shows the entropy versus the temperature for different values of the hybridization V, and the main panel shows the evolution of T^* and T_S, the temperature at which $S = \ln 2$, as a function of V. As expected, both temperature scales increase with increasing V with the same qualitative trend. T_S is lower than $T^\star$ in our calculations, because S includes a background contribution from free conduction electrons. In future work we intend to develop ways to isolate the entropy associated with magnetic correlations, and better test predictions[18] that $T_S \approx T^\star$.

Our DQMC simulations of the periodic Anderson model clearly capture key features found in NMR studies of heavy fermion materials, and provide a microscopic basis for the phenomenological two-fluid model. Our key conclusions are that (i) the temperature evolution of the susceptibility associated with different orbitals in this microscopic many-body Hamiltonian results in the Knight shift anomaly as observed experimentally; and (ii) the Knight shift results for different choices of interorbital hybridization and correlation energy in the localized orbital collapse onto a universal curve. This latter conclusion is especially intriguing since it suggests that heavy fermion materials can be described in a unified way, differing only through a distinct coherence temperature, T^*, controlled by the hybridization, V. Importantly, our results clearly reveal that the development of the heavy fermion state occurs over a broad temperature range below T^*, and also that both the local f-electrons as well as the itinerant quasiparticles contribute significantly to the NMR response over a broad range of hybridization values where non-Fermi liquid behavior has been observed. Further study of the spectral function $A(\omega)$, are in progress, and, in particular, whether $A(\omega)$ shows any change of behavior at the coherence temperature, as suggested recently by scanning tunneling microscopy [37].

[1] Z. Fisk, D.W. Hess, C.J. Pethick, D. Pines, J.L. Smith, J.D. Thompson and J.O. Willis, Science 239, 33 (1988).
[2] G.R. Stewart, Rev. Mod. Phys. 56, 755 (1984).
[3] J.D. Thompson, R. Movshovich, Z. Fisk, F. Bouquet, N.J. Curro, R.A. Fisher, P.C. Hammel, H. Hegger, M.F. Hundley, M. Jaime, P.G. Pagliuso, C. Petrovic, N.E. Phillips, and J.L. Sarrao, J. Magn. Magn. Mater. 226, 5 (2001).
[4] J.A. Mydosh and P.M. Oppeneer, Rev. Mod. Phys. 83, 1301 (2011).
[5] J. Custers, P. Gegenwart, H. Wilhelm, K. Neumaier, Y. Tokiwa, O. Trovarelli, C. Geibel, F. Steglich, C. Pepin, and P. Coleman, Nature 424, 524 (2003).
[6] P. Coleman and A.J. Schofield, Nature 433, 226 (2005).
[7] G.R. Stewart, Rev. Mod. Phys. 73, 797 (2001).
[8] T. Park, F. Ronning, H.Q. Yuan, M.B. Salamon, R. Movshovich, J.L. Sarrao, and J. D. Thompson, Nature 440, 65 (2006).
[9] B.L. Young, R.R. Urbano, N.J. Curro, J.D. Thompson, J.L. Sarrao, A.B. Vorontsov, and M.J. Graf, Phys. Rev. Lett. 98, 036402 (2007).
[10] M. Kenzelmann, Th. Strassle, C. Niedermayer, M. Sigrist, B. Padmanabhan, M. Zolliker, A.D. Bianchi, R. Movshovich, E.D. Bauer, J.L. Sarrao, and J.D. Thompson, Science 321, 1652 (2008).
[11] N.J. Curro, Rep. Prog. Phys. 72, 026502 (2009).
[12] N.J. Curro, B.L. Young, J. Schmalian, and D. Pines, Phys. Rev. B70, 235117 (2004).
[13] K.R. Shirer, A.C. Shockley, A.P. Dioguardi, J. Crocker, C.H. Lin, N. apRoberts-Warren, D.M. Nisson, P. Klavins, J.C. Cooley, Y.F. Yang, and N.J. Curro, Proc. Natl. Acad. Sci. 109, E3067 (2012).
[14] Y.F. Yang and D. Pines, Phys. Rev. Lett. 100, 096404 (2008).
[15] E. Kim, M. Makivic, and D.L. Cox, Phys. Rev. Lett. 75, 2015 (1995).
[16] T. Ohama, H. Yasuoka, D. Mandrus, Z. Fisk, and J.L. Smith, J. Phys. Soc. Jpn. 64, 2628 (1995).
[17] F. Mila and T.M. Rice, Phys. Rev. B40, 11382 (1989).
[18] Y.F. Yang and D. Pines, Proc. Natl. Acad. Sci. 45, E3060 (2012).
[19] A. M. Clogston, and V. Jaccarino, Phys. Rev. 121, 1357 (1961).
[20] J. Gan, P. Coleman, and N. Andrei, Phys. Rev. Lett. 68, 3476 (1992).
[21] S. Nakatsuji, D. Pines, and Z. Fisk, Phys. Rev. Lett. 92, 016401 (2004).
[22] Y.F. Yang and D. Pines, Phys. Rev. Lett. 100, 096404 (2008).
[23] Y.F. Yang, Z. Fisk, H.O. Lee, J.D. Thompson, and D. Pines, Nature 454, 611 (2008).
[24] J.R. Schrieffer and P.A. Wolff, Phys. Rev. 149, 491 (1966).
[25] M. Vekic, J. W. Cannon, D. J. Scalapino, R. T. Scalettar, and R. L. Sugar, Phys. Rev. Lett. 74, 2367 (1995).
[26] Carey Huscroft, A.K. McMahan, and R.T. Scalettar, Phys. Rev. Lett. 82, 2342 (1999).
[27] S. Doniach, Physica 91B, 231 (1977); B. Cornut and B. Coqblin, Phys. Rev. B5, 441 (1972).
[28] R. Blankenbecler, D.J. Scalapino, and R.L. Sugar, Phys. Rev. D24, 2278 (1981).
[29] The 'Trotter' error associated with the discretization of inverse temperature β is typically smaller than statistical errors from the Monte Carlo sampling, and can be eliminated by extrapolation.
[30] E.Y. Loh, J.E. Gubernatis, R.T. Scalettar, S.R. White, D.J. Scalapino, and R.L. Sugar, Phys. Rev. B41, 9301 (1990).
[31] The lack of flatness of $\chi_{cc}(T \to 0)$ expected from Pauli behavior at the smallest hybridization, $V = 0.5$, is associated with the van-Hove singularity in the density of states at half-filling of a tight binding, near-neighbor hopping, Hamiltonian on a square lattice.
[32] In the limit where $\chi_{cc}, \chi_{cf} << \chi_{ff}$, $B_{eff} = B$ and $K_{0\,eff} = K_0$. See Eq. 2.
[33] The choice of intra- vs. inter-site f-c hybridization affects the noninteracting band-structure. In the intrasite case, it exhibits a band-gap, while there is no gap in the inter-site case. The effect of these choices has been studied in the 'Kondo volume collapse' in cerium, where it does not alter the qualitative physics. See [35].
[34] M. Jarrell, Hossein Akhlaghpour, and Th. Pruschke, Phys. Rev. Lett. 70, 1670 (1993).
[35] K. Held, C. Huscroft, R.T. Scalettar, and A.K. McMahan, Phys. Rev. Lett. 85, 373 (2000).
[36] N. apRoberts-Warren, A. P. Dioguardi, A. C. Shockley, C. H. Lin, J. Crocker, P. Klavins, D. Pines, Y.F. Yang, and N. J. Curro, Phys. Rev. B83, 060408 (2011).
[37] P. Aynajian, E.H. da Silva Neto, A. Gyenis, R.E. Baumbach, J.D. Thompson, Z. Fisk, E.D. Bauer, and A. Yazdani, Nature 486, 201 (2012).